

# Increase in the amplitude of a saturated absorption resonance in an active interferometer

D.Yu. Primakov, P.V. Pokasov, S.N. Bagayev

**Abstract.** The behaviour of the amplitude of a saturated absorption resonance observed in laser radiation propagated through an active interferometer with nonlinear amplifying and absorbing media is studied experimentally for the first time. Upon variation of the gain in the amplifying medium and preserving a constant saturating field in the interferometer, a nonlinear increase in the amplitude of the saturated absorption resonance was observed. In this case, an increase in the detected signal exceeded an increase in the noise, i.e., the signal-to-noise ratio also increased.

**Keywords:** nonlinear optical resonance, laser spectroscopy, active interferometer, saturation, absorption.

## 1. Introduction

Modern methods of ultrahigh-resolution nonlinear laser spectroscopy [1, 2] allow one to study not only the homogeneous width of spectral lines broadened due to the Doppler effect but also to determine their centre with high accuracy. The latter circumstance is especially important for the development of optical frequency standards [3–6] because it permits one to relate directly the laser frequency to a quantum transition centre. The structure of absorption lines in low-pressure atomic and molecular gases has been studied by three widely used methods of nonlinear laser spectroscopy: saturation spectroscopy, two-photon spectroscopy, and spectroscopy in spatially separated fields. Another approach uses laser cooling and trapping of atoms and ions. This direction, which has been extensively developed in the last years [7], opens up fundamentally new possibilities for laser spectroscopy and metrology.

At the same time, the development of all the methods of nonlinear laser spectroscopy requires a sufficiently narrow-band laser radiation (with a high short-term frequency stability). A narrow laser line ( $\leq 1$  Hz) can be obtained by two methods. The first one is based on the stabilisation of the laser frequency with the help of a high- $Q$  interferometer [8, 9], while the second one uses the saturation spectroscopy

scheme, when the laser frequency is stabilised at the maximum of a narrow optical saturated absorption resonance [3] or saturated dispersion [4] in a low-pressure gas. The smaller the resonance width, the more accurately the laser frequency can be tuned to the resonance centre. However, to achieve the high short-term frequency stability, it is also very important to have the adequate resonance intensity (more exactly, the signal-to-noise ratio). The position of the resonance centre determines the long-term stability and reproducibility of the laser frequency. To achieve the high long-term stability and especially reproducibility of the laser frequency, very narrow resonances are required because in this case the influence of various physical and technical factors on the shift of the resonance and, hence, the stabilised laser frequency can be minimised.

The narrowing of resonances is accompanied by a drastic decrease in their intensity due to a decrease in the number of particles interacting with the field, which becomes a principal factor limiting the resolution of saturation spectroscopy. In fact, the problem of detecting weak signals and increasing the signal-to-noise ratio is the main problem for practical realisation of any of the above methods of nonlinear laser spectroscopy.

A saturated absorption resonance (inverted Lamb dip) appears in the resonance interaction of counterpropagating waves with a gas. The absorption coefficient for one of the travelling waves is

$$\alpha = \alpha_0 \exp\left(-\frac{\Omega^2}{\omega_D^2}\right) \left(1 - \frac{\kappa}{2} \frac{\Gamma^2}{\Omega^2 + \Gamma^2}\right),$$

where  $\Omega = \omega - \omega_{21}$  is the detuning of the wave frequency  $\omega$  with respect to the transition frequency  $\omega_{21}$ ;  $\omega_D$  is the Doppler line width;  $\Gamma$  is the homogeneous half-width of the line ( $\Gamma \ll \omega_D$ );  $\kappa$  is the saturation parameter proportional to the travelling wave intensity (here,  $\kappa \ll 1$ ); and  $\alpha_0$  is unsaturated absorption coefficient at the line centre. Under the condition  $\omega = \omega_{21}$ , a resonance with the homogeneous width is observed at the centre of the broadened Doppler absorption line.

The absorption resonance can be detected by measuring either the radiation power absorbed in the medium or the radiation energy scattered in the medium. The methods and schemes for detecting narrow optical resonances are described in detail in a number of monographs and reviews [1, 2, 10].

This work continues the experimental studies [11–13] of the shape of saturation absorption resonances observed in the transmission band of an active Fabry–Perot interferometer containing a nonlinearly absorbing gas cell. To our knowledge, the possibility of nonlinear amplification of the

D.Yu. Primakov, P.V. Pokasov, S.N. Bagayev Institute of Laser Physics, Siberian Branch, Russian Academy of Sciences, prospr. akad. Lavrent'eva 13/3, 630090 Novosibirsk, Russia;  
e-mail: dima@laser.nsc.ru, pokasov@laser.nsc.ru, bagayev@laser.nsc.ru

Received 9 January 2004; revision received 22 September 2004

Kvantovaya Elektronika 35 (2) 153–156 (2005)

Translated by M.N. Sapozhnikov

amplitude of saturated absorption resonances appearing in the field of a standing wave in an active interferometer with a nonlinear absorber was first reported in [12]. The amplitudes of saturated absorption resonances for passive and active interferometers with nonlinear absorption were compared using the elementary classical theory of a Fabry–Perot interferometer [13]. It was concluded that in the regime of differential amplification of the active interferometer, the amplitude of nonlinear resonances can be one–two orders of magnitude greater than that for the passive interferometer. A rigorous theoretical analysis [14] showed that the ‘useful’ signal in the active interferometer increases faster than noise, and the signal-to-noise ratio can be more than an order of magnitude greater than that in the passive interferometer.

## 2. Experimental

Saturated absorption resonances were investigated at a wavelength of  $3.39\text{ }\mu\text{m}$ . A He–Ne laser with an intracavity methane cell operating below the lasing threshold was used as an active interferometer. The active interferometer (Fig. 1) had a symmetric  $\Pi$ -shaped configuration formed by two plane fold mirrors (with the reflectivity  $r \geq 0.98$ ), which were mounted at an angle of  $45^\circ$  to the optical axis, by two semi-transparent mirrors for radiation input and output.

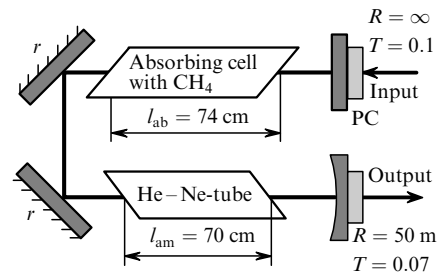


**Figure 1.** Scheme of the active interferometer ( $l_{ab}$ : absorbing cell length,  $l_{am}$ : discharge gap length in the amplifying tube; PC: piezoelectric ceramics; the resonator length is 180 cm).

The general scheme of the experimental setup is shown in Fig. 2. The radiation frequency  $v_{st}$  of the reference laser was stabilised by the absorption saturation resonance in methane, whose half-width was  $\sim 50\text{ kHz}$ . The system for automatic frequency control (AFC 1) was an extremal control system with a probe sinusoidal modulation signal at a frequency of 15 kHz operating by the zero signal of the first harmonic in the reference laser output power. The relative frequency instability of the reference laser (the Allan parameter) changes linearly with the slope  $10^{-14}/\tau^{1/2}$  at the averaging times  $\tau = 0.01 – 10\text{ s}$ , and remains no worse than  $10^{-14}$  up to  $\tau = 10^3\text{ s}$  [15]. The absolute value of the

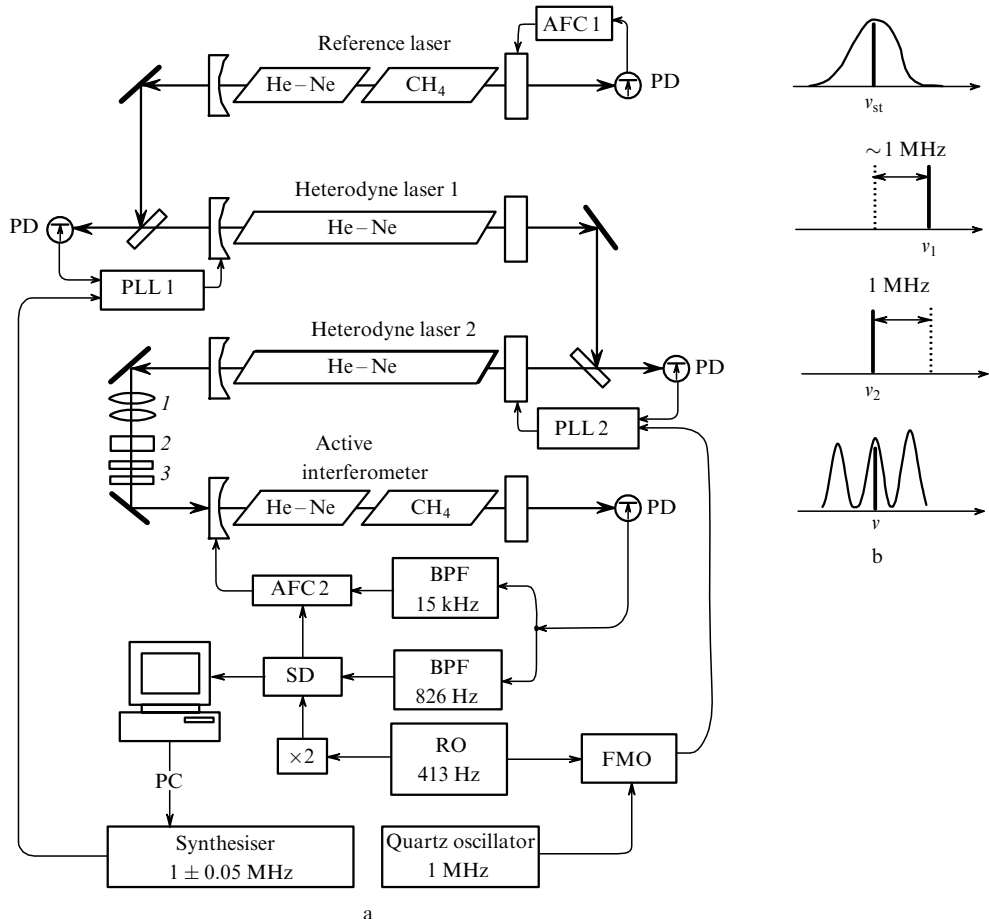


**Figure 2.** Scheme of the experimental setup (a) and positions of optical frequencies (b): (1) matching optics; (2) Faraday isolator; (3) calibrated attenuators; (RO) radio-frequency oscillator; (PD) photodetector; (BPF) band path filter; (SD) synchronous detector; (AFC 1 and AFC 2) automatic frequency control systems; (PLL 1 and PLL 2) phase-locked loop systems; (FMO) frequency-modulated oscillator.

frequency  $v_{st}$  usually exceeds the frequency of the  $F_2^{(2)}P7v_3$  absorption line of methane by  $2 \pm 0.5$  kHz, which was verified in many independent experiments.

Two additional heterodyne lasers used in the experimental setup allow us to obtain stable and broadly tunable radiation for excitation of the active interferometer. The radiation frequency  $v_1$  of the first heterodyne laser was synchronised in phase with the radiation frequency of the reference laser with the help of the phase-locked loop system (PLL 1). This permits the transfer of the frequency characteristics of reference radiation to the heterodyne laser almost without losses and shifts the difference frequency between them from the region of zero beats. The initial shift  $v_1 - v_{st} \approx 1$  MHz is specified by a controlled synthesiser, which serves as a reference oscillator for the PLL 1 system. The frequency  $v_2$  of the second heterodyne laser is maintained with the PLL 2 system so that the condition  $v_1 - v_2 = 1$  MHz is preserved in the case of phase matching of frequencies  $v_2$  and  $v_1$ . The length of the active interferometer was stabilised with the help of the AFC 2 system, which is similar to the AFC 1 system, in such a way that the centre  $v$  of the transmission band was always coincident with the frequency  $v_2$  of the input radiation. The tuning of the synthesiser frequency allows us to control the frequency  $v_1$  and, hence, the frequency  $v_2$  and to record the absorption line shape. The range and step of the synthesiser tuning are specified with the software.

The saturated absorption resonance was detected by the method of synchronous detection of the second-harmonic signal in the radiation power transmitted through the active interferometer. The radiation incident on the interferometer was modulated at the frequency 413 Hz with a frequency-modulated oscillator (FMO), which was the reference oscillator for the PLL 2 system. The average FMO frequency was specified by a quartz oscillator.

### 3. Experimental results

A key factor in the observation of saturated absorption resonances in an external interferometer is the  $Q$  factor of the latter. An increase in the  $Q$  factor leads to an increase in the effective absorption length and an increase in the amplitude of a detected signal. In the case of a passive interferometer, the  $Q$  factor is constant and is mainly determined by losses in an absorbing medium and at the interferometer mirrors. The  $Q$  factor of an active interferometer can be regulated and depends on the gain in its active medium. In the scheme presented in Fig. 1, the FWHM  $\Delta v$  of the transmission band of the active interferometer was  $\sim 4.7$  MHz (the finesse was  $F \approx 18$ ) when the amplifying He–Ne tube was switched off and the methane pressure was  $p_{\text{CH}_4} \approx 10^{-4}$  Torr. When the gain was switched on, the transmission band of the active interferometer narrowed down to  $\sim 50$  kHz ( $F \approx 1700$ ). A further narrowing of the transmission band was limited by the accuracy of approaching the self-excitation threshold of the interferometer and was determined by instability of the current of the high-voltage power supply of the amplifying He–Ne tube.

We studied the dependence of the amplitude of saturated absorption resonances on the  $Q$  factor of the active interferometer. The  $Q$  factor was varied by changing the discharge current in the He–Ne tube. A change in the  $Q$  factor was quantitatively estimated by measuring the width

of the transmission band of the active interferometer. The saturating power in the interferometer was maintained constant with the help of calibrated attenuators placed in front of the interferometer. The experiment was performed for two different methane pressures in the absorbing cell of the active interferometer.

The obtained experimental dependences are presented in Fig. 3. Upon the narrowing of the transmission band of the active interferometer, the amplitude of the saturated absorption resonance increased nonlinearly. As the self-excitation threshold of the interferometer is approached, the slope of the experimental curves sharply increases and repeats the main features of the dependence (Fig. 4) calculated using the model [11]. We did not attempt to observe resonances when the amplifying He–Ne tube was switched off because the power of external radiation was insufficient to produce in the interferometer the same saturating field as in the active regime.

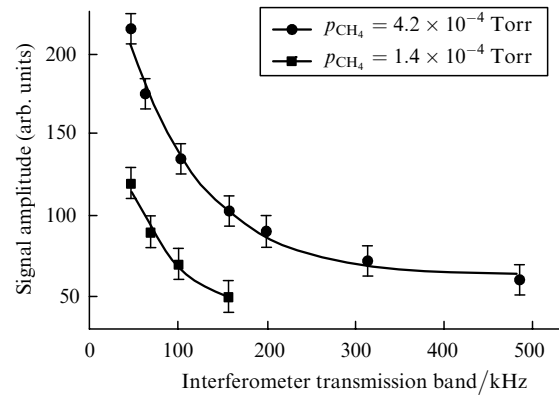


Figure 3. Dependences of the amplitude of the saturated absorption resonance in methane on the  $Q$  factor of the active interferometer.

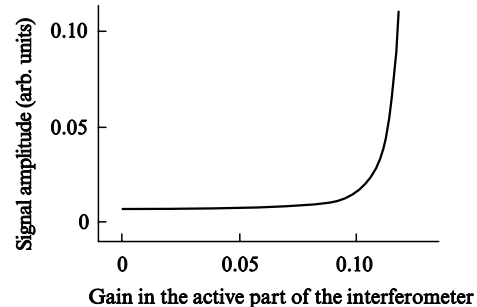
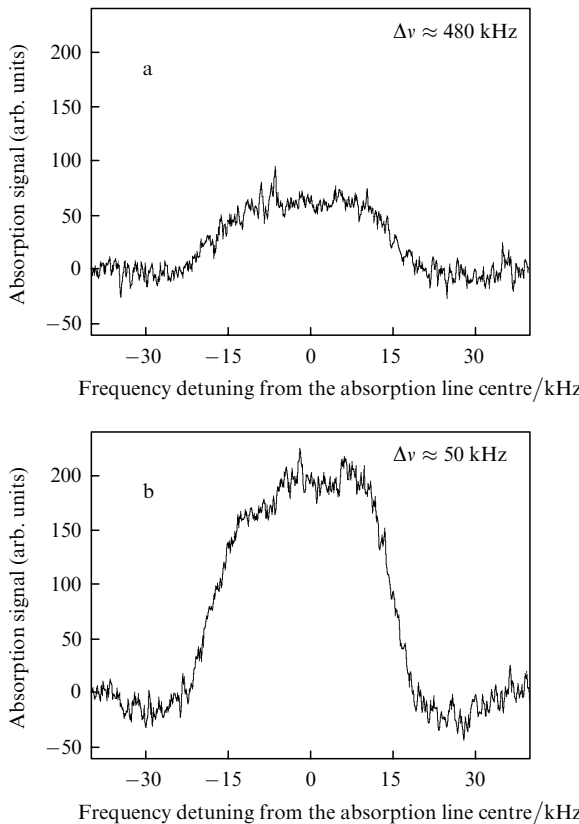


Figure 4. Theoretical dependence of the amplitude of a saturated absorption resonance in the active interferometer on the dimensionless gain in the He–Ne tube. The increase in the gain corresponds to the narrowing of the transmission band of the active interferometer.

Note that, as the self-excitation threshold of the active interferometer is approached, both the saturated absorption signal and noise will increase. The behaviour of the signal-to-noise ratio in this case was analysed in detail in theoretical paper [14]. The quantum fluctuations of external radiation were considered as the noise source. It was shown that, as the  $Q$  factor of the active interferometer increased, the ‘useful’ signal increased faster than noise, and the signal-to-noise ratio near the self-excitation threshold could increase by more than an order of magnitude.

This conclusion was qualitatively confirmed in our experiment. Saturated absorption resonances were detected with an InSb photodetector cooled by liquid nitrogen. The intrinsic noise of the photodetector was a few times lower than the noise of incident radiation. For comparison, Fig. 5 shows the second harmonic form of nonlinear absorption resonances recorded for  $p_{\text{CH}_4} \approx 4.2 \times 10^{-4}$  Torr and the transmission bands of the active interferometer  $\Delta\nu \approx 480$  and 50 kHz. One can see that the increase in the signal noticeably exceeds that of the noise, in accordance with theoretical conclusions [14]. As a result, the resolution improves, which is manifested in a greater asymmetry of the resonance shape (Fig. 5b) demonstrating the presence of the three components of the hyperfine structure of the  $F_2^{(2)}$  line of methane. By comparing the amplitudes of signals in Figs 5a, b and the corresponding noise dispersions, we estimated the increase (approximately threefold) in the signal-to-noise ratio obtained in this case. The signal-to-noise ratio was also increased with increasing the  $Q$  factor of the active interferometer for  $p_{\text{CH}_4} \approx 1.4 \times 10^{-4}$  Torr.



**Figure 5.** Experimental curves of the saturated absorption resonance in methane recorded for different  $Q$  factors of the active interferometer (the time constant of the synchronous detector is  $\tau = 1$  s, the frequency detuning step is 117 Hz).

#### 4. Conclusions

By using the laser spectrometer based on the active interferometer, we have studied the dependence of the amplitude of a saturated absorption resonance on the  $Q$  factor of the active interferometer.

The passive interferometer can be treated as a system with a specified  $Q$  factor, which is determined by losses at

mirrors and absorption. An amplifying medium placed in the interferometer allows the control of its  $Q$  factor and provides an increase in the amplitude of saturated absorption resonances. The experimental increase in the signal amplitude with increasing the  $Q$  factor agrees with the theoretical calculation. The experimental results confirm the theoretical conclusion [14] that the signal-to-noise ratio in the active interferometer can be increased compared to that in the passive interferometer.

In our opinion, the active interferometer with a saturable absorber is promising for applications in nonlinear spectroscopy and laser frequency stabilisation.

**Acknowledgements.** The authors thank A.K. Dmitriev and A.A. Kurbatov for useful discussions. This work was supported by the Russian Foundation for Basic Research (Grant No. 02-02-16464-a).

#### References

1. Letokhov V.S., Chebotayev V.P. *Nelineinaya lazernaya spektroskopiya sverkhvysokogo razresheniya* (Nonlinear Laser Ultrahigh-resolution Spectroscopy) (Moscow: Nauka, 1990).
2. Demtröder W. *Laser Spectroscopy* (Berlin, Heidelberg, New-York: Springer-Verlag, 1996).
3. Bagayev S.N., Chebotayev V.P. *Usp. Fiz. Nauk.*, **148**, 143 (1986).
4. doi> 4. Gubin M.A., Protsenko E.D. *Kvantovaya Elektron.*, **24**, 1080 (1997) [*Quantum Electron.*, **27**, 1048 (1997)].
5. Basov N.G., Gubin M.A. *IEEE J. Select. Top. Quantum Electron.*, **6** (6), 857 (2000).
6. Baklanov E.V., Pokasov P.V. *Kvantovaya Elektron.*, **33**, 383 (2003) [*Quantum Electron.*, **33**, 383 (2003)].
7. Eschner J., Morigi G., Schmidt-Kaler F., Blatt R. *J. Opt. Soc. Am. B*, **20**, 1003 (2003).
8. Drever R.W.P., Hall J.L., Kowalski F.V., Hough J., Ford G.M., Munley A.J., Ward H. *Appl. Phys. B*, **31**, 97 (1983).
9. Young B.C., Cruz F.C., Itano W.M., Bergquist J.C. *Phys. Rev. Lett.*, **82**, 3799 (1999).
10. Ye J., Ma L-S., Hall J.L. *J. Opt. Soc. Am. B*, **15**, 6 (1998).
11. Pokasov P.V., Primakov D.Yu., Bagayev S.N. *Proc. SPIE Int. Soc. Opt. Eng.*, **4900**, 167 (2002).
12. Ostromensky M.P., Pokasov P.V., in *Aktual'nye voprosy teplofiziki i fizicheskoi gidrogazodinamiki* (Topical Problems of Thermal Physics and Physical Fluid Gas Dynamics) (Novosibirsk: Izd. Institute of Thermal Physics, Siberian Branch, RAS, 1991) p. 290; Pokasov P.V., Ostromensky M.P. *Tezisy dokladov mezhdunarodnoi konferentsii 'Optika lazerov-93'* (Abstracts of Papers, Int. Conf. on Laser Optics-93) (Saint Petersburg, 1993) p. 308.
13. Bagayev S.N., Pokasov P.V. *Laser Phys.*, **10**, 894 (2000).
14. Bagayev S.N., Kurbatov A.A., Titov E.A. *Laser Phys.*, **11**, 1313 (2001).
15. Bagayev S.N., Dmitriev A.K., Pokasov P.V. *Laser Phys.*, **7**, 989 (1997).